

Optimization of YOLOV7’s hyper parameters for simultaneous object detection in satellite imagery

Abhimanyu Singh¹ and Manisha Nene J¹

¹Defence Institute of Advanced Technology

February 1, 2023

Abstract

Object detection is crucial for computer vision applications that use satellite imagery, such as precision agriculture, urban planning, and military applications. Recognizing objects in satellite images is challenging due to numerous factors, including the sheer number of objects, the variety in their positions, the range in their sizes, the quality of the lighting, and the existence of a dense background. Background complexity, differences in data capture geometry, geography, and illumination, and an abundance of different types of objects all contribute to making automatic detection in satellite images particularly difficult. There have been many advancements in object detection methods over time, including YOLO and its variations, CNN and its offshoots, DETR and its offshoots, and so on; nonetheless, it is still required to test these methods on the requisite data set to determine their true efficacy. Researchers have investigated the idea of autonomously detecting structures, automobiles, and other things to reduce the risk of human error and speed up the procedure. Improvements in deep learning algorithms and hardware systems have allowed us to accurately identify a broader range of objects in ultra-high-resolution satellite imagery. Through parameter adjustment and analysis of results on the Xview dataset, we determine the most effective technique for multiple item detection and compare it to other models.

Optimization of YOLOV7’s hyper parameters for simultaneous object detection in satellite imagery

Abhimanyu Singh* and Manisha J Nene**

School of Computer Engineering and Mathematical Sciences

Defence Institute of Advanced Technology, Pune

* *abhiman_pce@yahoo.co.in*

** *mjnene@diat.ac.in,*

Abstract— Object detection is crucial for computer vision applications that use satellite imagery, such as precision agriculture, urban planning, and military applications. Recognizing objects in satellite images is challenging due to numerous factors, including the sheer number of objects, the variety in their positions, the range in their sizes, the quality of the lighting, and the existence of a dense background. Background complexity, differences in data capture geometry, geography, and illumination, and an abundance of different types of objects all contribute to making automatic detection in satellite images particularly difficult. There have been many advancements in object detection methods over time, including YOLO and its variations, CNN and its offshoots, DETR and its offshoots, and so on; nonetheless, it is still required to test these methods on the requisite data set to determine their true efficacy. Researchers have investigated the idea of autonomously detecting structures, automobiles, and other things to reduce the risk of human error and speed up the procedure. Improvements in deep learning algorithms and hardware systems have allowed us to accurately identify a broader range of objects in ultra-high-resolution satellite imagery. Through parameter

adjustment and analysis of results on the Xview dataset, we determine the most effective technique for multiple item detection and compare it to other models.

Index Terms — Object Detection, YOLO, TP, Deep Learning, Machine Learning, mAP, PR AUC, F1 AUC.

1. Introduction

Object identification is a crucial computer vision problem used to identify specific kinds of visual things (such people, animals, cars, or buildings) inside a given digital image. The primary focus of object detection research is the creation of computational models that supply the bare minimum of data required by computer vision applications. Object detection using satellite images is extremely useful in many different fields, including defence and military applications, urban studies, airport surveillance, vessel traffic monitoring, and the determination of transportation infrastructure. Object detection provides the foundation for a wide variety of subsequent computer vision tasks, such as instance segmentation, image captioning, object tracking, and many others. Detecting pedestrians, animals, vehicles, people, text, poses, licence plates, and numbers are just a few examples of the many ways object detection can be put to use. Object detection may be broken down into its component parts, which include categorising things and pinpointing their locations in pictures. Thus far, research efforts have been split towards optimising either one of these activities independently or both of them jointly [1][2]

If satellite photos are our data, then the metadata that characterise them are our "data for the data." When did you take these pictures? How did the sensor's geometry look like back then? In what part of the Earth does this picture take place? These kinds of questions are answered by the metadata Imagery of Earth captured by imaging satellites owned and controlled by governments and corporations throughout the world are referred to variously as satellite photographs, Earth observation imagery, spaceborne photography, and satellite photos. Images captured by satellites are taken from great heights, thus they are subject to atmospheric interference, viewpoint shifts, clutter in the background, and lighting changes. As a result, satellite-collected remote sensing images are much more complicated than computer vision images.. Furthermore, in comparison to digital pictures produced from cameras, satellite images cover wider regions and reflect the complex terrain of the Earth's surface (various land types) with two-dimensional images with less spatial information.

Satellite photos have a larger data size and geographical coverage than natural photographs. Still commonly utilised in satellite-based object detection research is a visual interpretation technique that makes use of expert knowledge to distinguish between potential objects/targets. Since it is manual, this method is slow and relies on a high level of experience to get accurate results. Research on automatic target identification—including buildings, planes, ships, etc.—has been pursued for some time in an effort to minimise human mistake and expedite the process. However, automated detection is difficult for satellite pictures because of the intricacy of the backdrop, variances in data collecting geometry, geography, and lighting conditions, and the variety of objects.[3][4] In particular, deep neural networks have proven useful for object identification, and it is now clear that optimising their learning process is a matter of selecting the appropriate hyperparameters. This is done by hyperparameter optimization by the application of genetic algorithms.

Experiments are conducted to implement a genetic algorithm to find the right hyperparameters, and then another experiment compares the performance of the optimal and original deep learning model using the performance metrics mentioned in the study. The study begins with a literature review to identify the most effective deep learning techniques for object detection in satellite and aerial images. The main aim behind training module is to train and develop the AI model using custom learning techniques to enable automatic detection and classification of customized objects in the satellite imagery.

The outline of the article is to develop a model to overcome the challenges of object detection and images formed through satellite. The article establishes a goal function that measures the deviation between the actual and target values for the vector output. The inaccuracy in this computation is minimised by having

the computer adjust certain internal settings (weights or actual numbers). Millions of weights are employed in deep learning’s training process. Therefore, the gradient vector is applied to each weight vector to indicate the decline and rise in error. The findings of the literature study indicate that the deep learning approaches are the most effective ones for object detection in satellite and aerial photos.

2 RELATED WORK

Researchers on both sides of the Atlantic have classified the most popular methods of object recognition into three broad groups: those that utilise motion data, those that rely on feature extraction, and those that employ template matching. Most of the first research relied on unsupervised techniques and a wide variety of characteristics. In detection from panchromatic pictures was constructed using the scale-invariant feature transformed (SIFT) key points and the graph theorem. The unsupervised approaches were successful for a restricted set of objects, but they yielded efficient results for basic structure types in general. More recent research has centred on supervised learning techniques for accurately identifying objects of varying structures in challenging settings. Supervised learning achieves better results because, during training, it is applied to data that has already been annotated by hand.

Various supervised learning approaches utilising specially generated features were used before the mainstream adoption of convolutional neural network (CNN) architectures. Detecting objects is a two-stage procedure that uses motion and a convolutional neural network trained on patches (CNN). As a preliminary step, a lightweight motion detecting operator is used to approximate where the targets are.[7]

The second phase employs this data alongside a convolutional neural network to improve the detection accuracy. While Qinhan et al [15] use of many windows with high item probabilities and subsequent SVM and HOG algorithms for proposal generation has its advantages; the use of fixed-size windows is a significant drawback. In order to identify objects in UAV photographs, Lee et al. [8] used RCNN. A solution for vehicle detection based on the YOLO deep learning framework is proposed by Junyan Lu et al. [11]. With the use of deep learning, B.Cui et al [12] suggested targeted improvements based on the powerful YOLO v5 to improve the detection performance of small objects finding objects in satellite photos using this technique.

They applied the Faster RCNN-based RetinaNet framework on the COCW dataset. Surface-to-air missile (SAM) locations can be pinpointed with the help of a sliding window methodology for satellite imagery, as suggested by Marcum et al. [14]. The advent of deep learning and GPU technology has allowed for rapid and efficient progress in the field of computer vision, particularly when it comes to tackling challenges in pattern recognition and picture processing. With its ability to automatically extract characteristics from a picture, deep learning techniques play a crucial role in the field of object recognition. When it comes to detecting objects, deep learning excels. First, we need to gather the massive dataset and begin training on this dataset if we want to detect category. After training, we feed in a picture for prediction, and the model spits out category-specific score vectors.

It was proposed by Qian et al. (2020) to maximise the training of tiny objects without overlapping bounding boxes using a variant of Faster-RCNN with a new architecture, new metric, and loss. The findings of the studies demonstrate that the genetic algorithm was effective in determining the optimal values for the hyperparameters. When it came to the detection of aeroplanes, vehicles, and ships, the accuracy attained by improved models was significantly greater than that of the original models. The findings also indicate that the training timeframes for the models have been shortened thanks to the application of appropriate hyperparameters; however this has resulted in a minor loss of precision when it comes to the detection of ships.

3 PRELIMINARIES

3.1 Notations & Parameters

The parameters defined for training the model are:

- **Img:** set the size of the incoming image.
- **Batch:** figure out how many items to make at once.
- **Epochs:** set the training epoch count.
- **Data:** provide the location of yaml file.
- **Configuration file (cfg):** allows defining how our model will operate.
- **Weights :** Specify a non-standard location for the weights.
- **Learning rate (lrf):** optimising algorithm's tuning parameter that controls the size of the step taken at each iteration on the way to the loss functions minimum.
- **Momentum:** A new feature of the gradient descent optimization technique allows the search to gain momentum in a chosen direction, allowing it to glide over the search space's flat areas and avoid the pitfalls of erratic gradients.
- **Warmup-echos:** By providing more varied instances later in training, the "warm-up" helps mitigate the "primacy impact" of the initial set. Without it, the models will un-train those early superstitions, which could add a few epochs of run time before you reach the necessary convergence.
- **Weight decay:** machine learning regularisation strategy for simplifying models and avoiding overfitting.
- **Warmup- bias:** When an algorithm is biased, the outcome is skewed in favour of or against a particular notion. An inaccurate assumption made during the machine learning process can lead to bias, which is a type of systematic inaccuracy.

3.2 xView Data set

Over 1 million objects in 60 classes are spread out throughout over 1,400 km² of footage, making xView one of the largest and most diversified object recognition datasets accessible. Imagery with a better resolution is available in the xView dataset, which was compiled using data gathered from WorldView-3 satellites at a ground sample distance of 0.3m. There are a total of 60 classes in the dataset. Naming a few of them include 'Fixed-wing Aircraft', 'Small Aircraft', 'Cargo Plane', 'Helicopter', 'Passenger Vehicle', 'Small Car', 'Pickup Truck', 'Utility Truck', 'Truck' etc.

3.3 Single Stage Object Detectors

Object Detection in One Step models are a type of object detection models that only require a single pass through the detection process, as opposed to the two passes required by two-stage models. Typically, inference times are reduced in these models. Both the bounding boxes and the class probabilities within them are predicted by a single convolutional network.

3.4 YOLO V 5

The YOLO v5 has the same three essential components as any other single-stage object detector, model backbone, model head and model neck. Model Backbone is mainly used to extract important features from the given input image.[21][22][23]. The Cross Stage Partial Networks constitute the backbone of YOLO v5, which is utilised to extract highly informative features from an input picture.

Most of the time, Model Neck is used to make feature pyramids. Feature pyramids make it easier for models to generalise well about scaling of objects. With different sizes and scales, it helps to find the same thing. Feature pyramids are very helpful, and they help models do well with data they haven't seen before. Other

models, like FPN, BiFPN, PANet, etc. use different types of feature pyramid techniques. PANet is utilised as the neck in YOLO v5 to obtain the feature pyramids. Model Head is mostly employed in the latter stage of detection. It creates class probabilities, objectness scores, and bounding boxes in the form of a final output vector by applying anchor boxes to the features.

4. PROPOSED TECHNIQUE

4.1 Labelling Of Data

If an annotation's bounding box was divided over tiles, the ability to name the tiled pictures was built into the tiling script so that the photos could still be seen as a whole. The images are split in the ratio of 90:10 for our training and validation set respectively. The images from both the sets were further tiled as per memory allocation of both our models as 512x512. The annotations are split with the dimensions according to the image splits and scaled relatively for making it compatible with the YOLO framework. Each training iteration / experiment consisted of 30 epochs each to maintain the consistency.

Parameter Training & Tuning

```
Exp 1- python train.py -img 512 -batch 12 -noval -epochs 30 -data data/custom.yaml -weights yolov5m.pt -cfg models/yolov5m_custom.yaml -hyp data/hyps/hyp.scratch-med.yaml -device 0 -name ./experiment_x
```

Annotation of Image

Figure 1 shows the sample of an annotated image for the model. The steps involved in the annotation of the image are as under:

Step1: Download the xView dataset from <https://challenge.xviewdataset.org>.

Step 2: Split all the images in the ratio of 90:10 for our training and validation set respectively.

Step 3: Images from both the sets were further tiled as per memory allocation of models, i.e 512x512 for Yolo v5.

Step 4: The annotations were converted from GeoJSON Polygon objects to YOLO format using a script. We also split the annotations dimensions according to the image splits.

Step 5: The tiled dataset was further used to experiment and train our YOLO models. Each training iteration / experiment consisted of 30 epochs each to maintain the consistency between all models.



Fig 1. Annotated Image

5. EXPERIMENT SETUP & OBSERVATIONS

System Configuration

The system with the following configuration was used for the experiments and model building

- Intel Core i5-12100F
- Nvidia RTX 3050 8 GB
- 16 GB x 2 RAM @ 3200 MHz
-

Training the model using SGD Optimizer

Case1 (a). All paramaters kept at default value and using SGD optimizer

1. $lr0 \rightarrow 0.1$
2. $momentum \rightarrow 0.9$
3. $lrf \rightarrow 0.2$
4. $weight_decay: 0.0005$
5. $warmup_epochs: 3.0$
6. optimizer : SGD

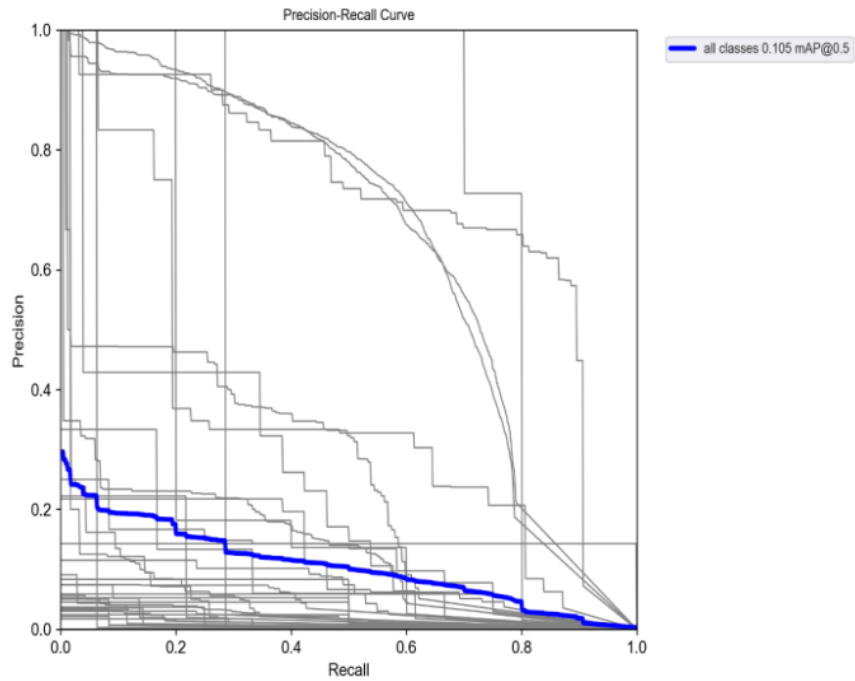
If ($\text{current learningrate} \geq \text{learning-rate-end}$):

Stop training

else

Continue training

In the first experiment the model is trained using the SGD optimizer. The value of the optimizer is kept at 0.01 to achieve the baseline evaluation model to carry out further comparison. The experiment is conducted with 30 epochs on the sub-sampled tiles of xView dataset. PR AUC 0.105 at mAP@0.5 | F1 max 0.09 at 0.114 confidence is achieved on the experiment and further tuning is conducted with taking this result as the baseline model. Figure 2 and Figure 3 shows the F1-Confidence curve and the Precision-Recall curve respectively.



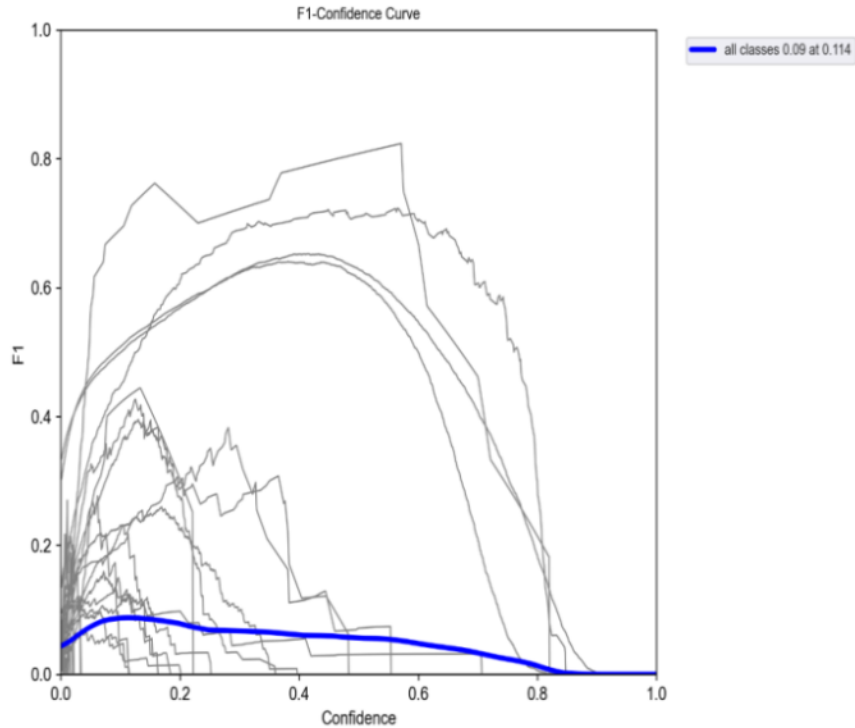


Figure 2: F1-Confidence Curve Fig 3: Precision- Recall curve

5.2 Training the model using ADAM Optimizer

Case1 (b). All paramaters kept at default value and keechanging the optimizer to ADAM.

1. $lr0 \rightarrow 0.1$
2. $momentum \rightarrow 0.9$
3. $lrf \rightarrow 0.2$
4. $weight_decay: 0.0005$
5. $warmup_epochs: 3.0$
6. optimizer : ADAM

In the second experiment the model is trained using the ADAM optimizer. The value of the optimizer is kept at 0.01 to evaluate if the model works better than SGD optimizer. The experiment is conducted with 30 epochs on the sub-sampled tiles of xView dataset. PR AUC 0.043 at mAP@0.5 | F1 max 0.03 at 0.071 confidence is achieved on the experiment and it is concluded that the model did not show better performance. Figure 2 and Figure 3 shows the F1-Confidence curve and the Precision-Recall curve respectively. Figure 4 shows the predicted objects in the image with their percentage of depiction.

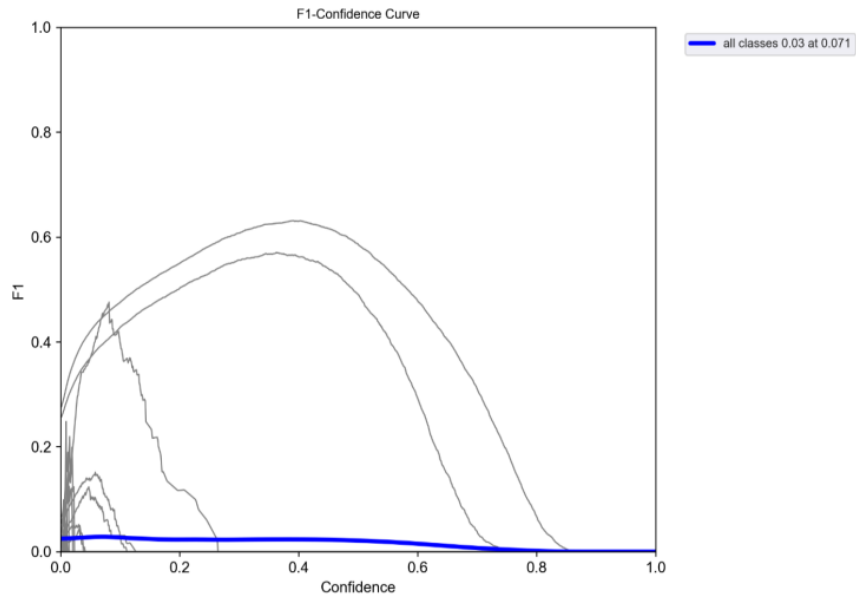
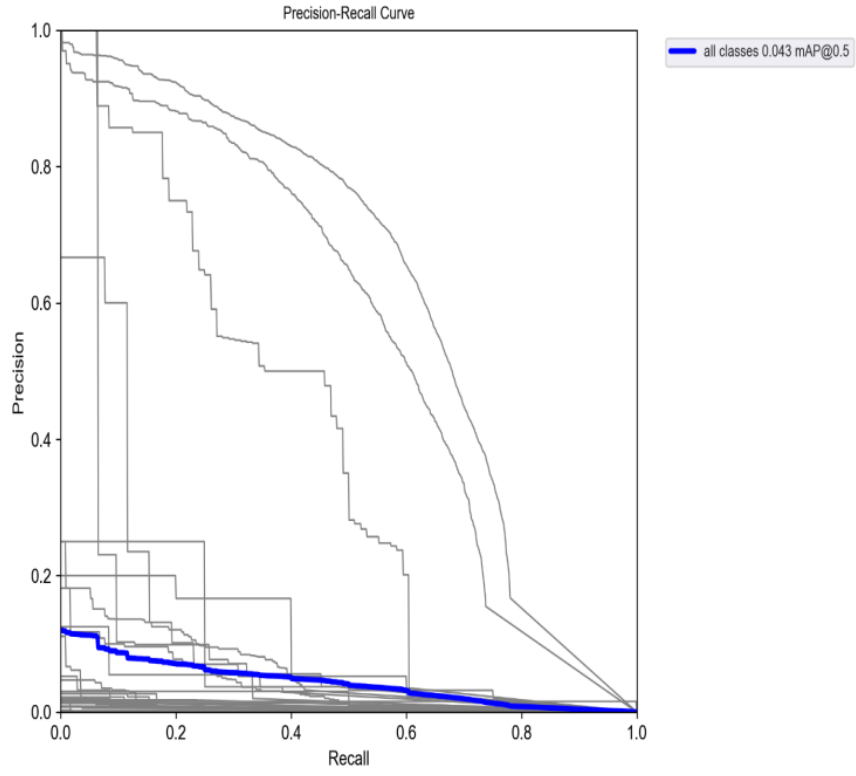


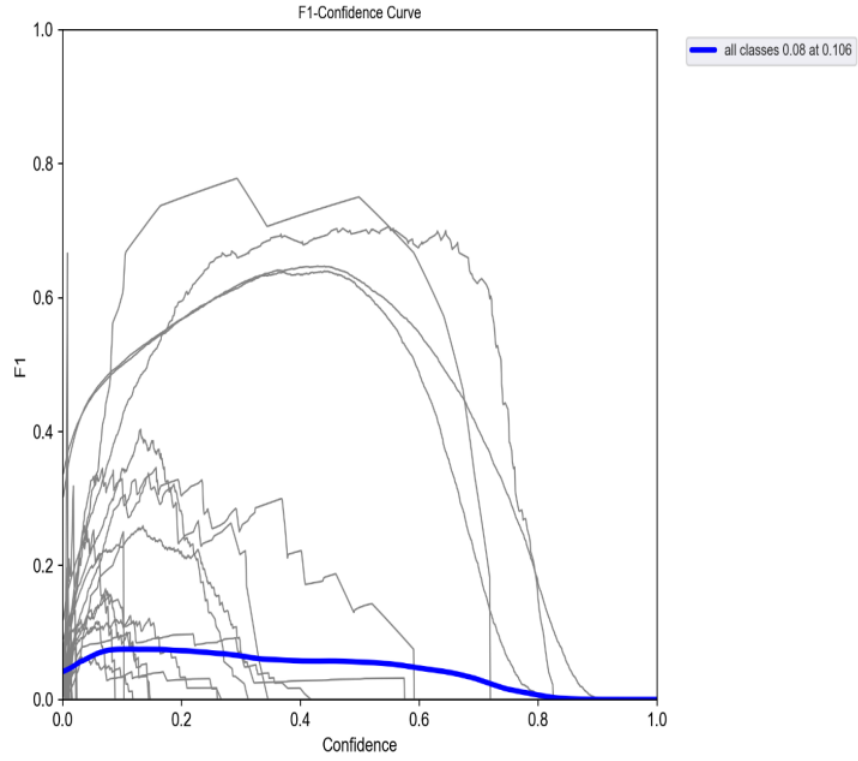
Fig 4: F1-Confidence Curve of ADAM optimizer Fig 5: Precision- Recall curve ADAM optimiser

5.3 Increase the momentum of SGD Optimiser

Case 2. Changing the value of momentum to 0.92

1. *lr0* -> 0.1
2. *momentum* ->0.92
3. *lrf* ->0.2
4. *weight_decay*: 0.0005
5. *warmup_epochs*: 3.0
6. *optimizer* : *SGD*

In this experiment, we increase the momentum slightly to see if performance can be improved. We increase the SGD momentum of our model to 0.92 to verify if increasing the momentum helps in getting better results. It was conducted with 30 epochs on the sub-sampled tiles of xView Dataset. PR AUC 0.104 at mAP@0.5 | F1 max 0.08 at 0.106 confidence was achieved and it was concluded that the model was not able to improve upon the performance. Figure 6 shows the F1-Confidence curve which depicts the score of F1 max 0.08 at 0.106 confidence rate which is very less. Figure 7 shows the Precision- Recall curve which depicts the score of AUC 0.104 at mAP@0.5 which is very less as compared to SGD momentum.



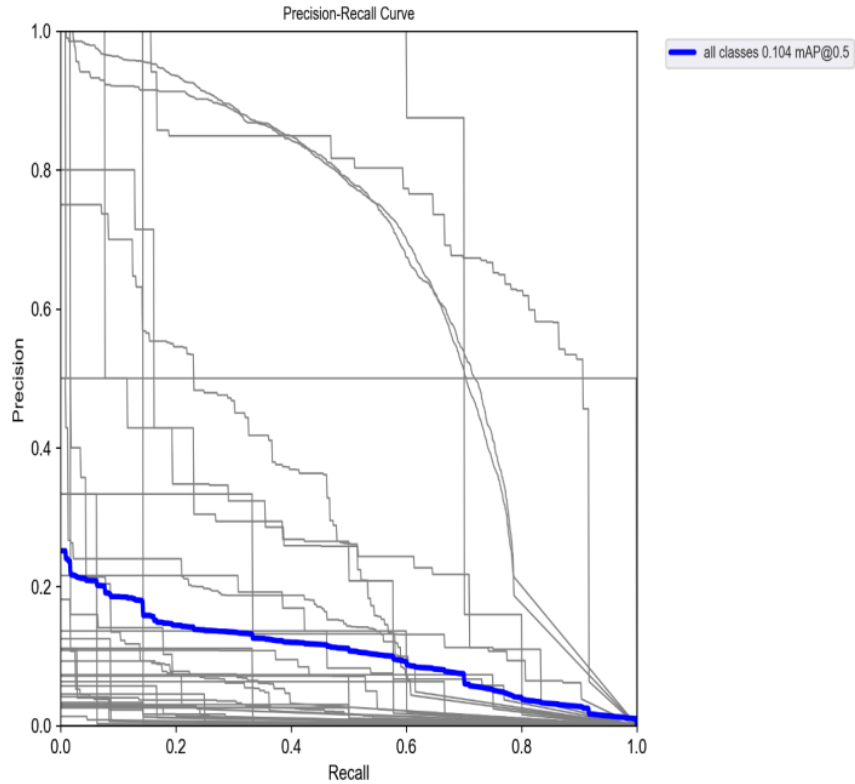


Fig 6: F1-Confidence Curve of increased momentum Fig 7: Precision- Recall Curve of increased momentum

5.4 Reduction in warmup echos in SGD Optimiser

Case 3. Changing the value of warm-up echos to 2.5

1. $lr0 \rightarrow 0.1$
2. $momentum \rightarrow 0.92$
3. $lrf \rightarrow 0.2$
4. $weight_decay: 0.0005$
5. $warmup_epochs \rightarrow 2.5$
6. $optimizer : SGD$

Reverting back to the best momentum that we found and reduce the warmup epochs to 2.5 to see if performance can be improved or helps in achieving better results. The experiment was conducted with 30 epochs on the sub-sampled tiles of xView Dataset. The result achieved was at a score of PR AUC 0.109 at mAP@0.5 | F1 max 0.09 at 0.095 confidences and were able to improve upon the performance on a lower scale. Figure 8 depicts the score of F1 max 0.09 at 0.095 confidence rate which is comparatively good.

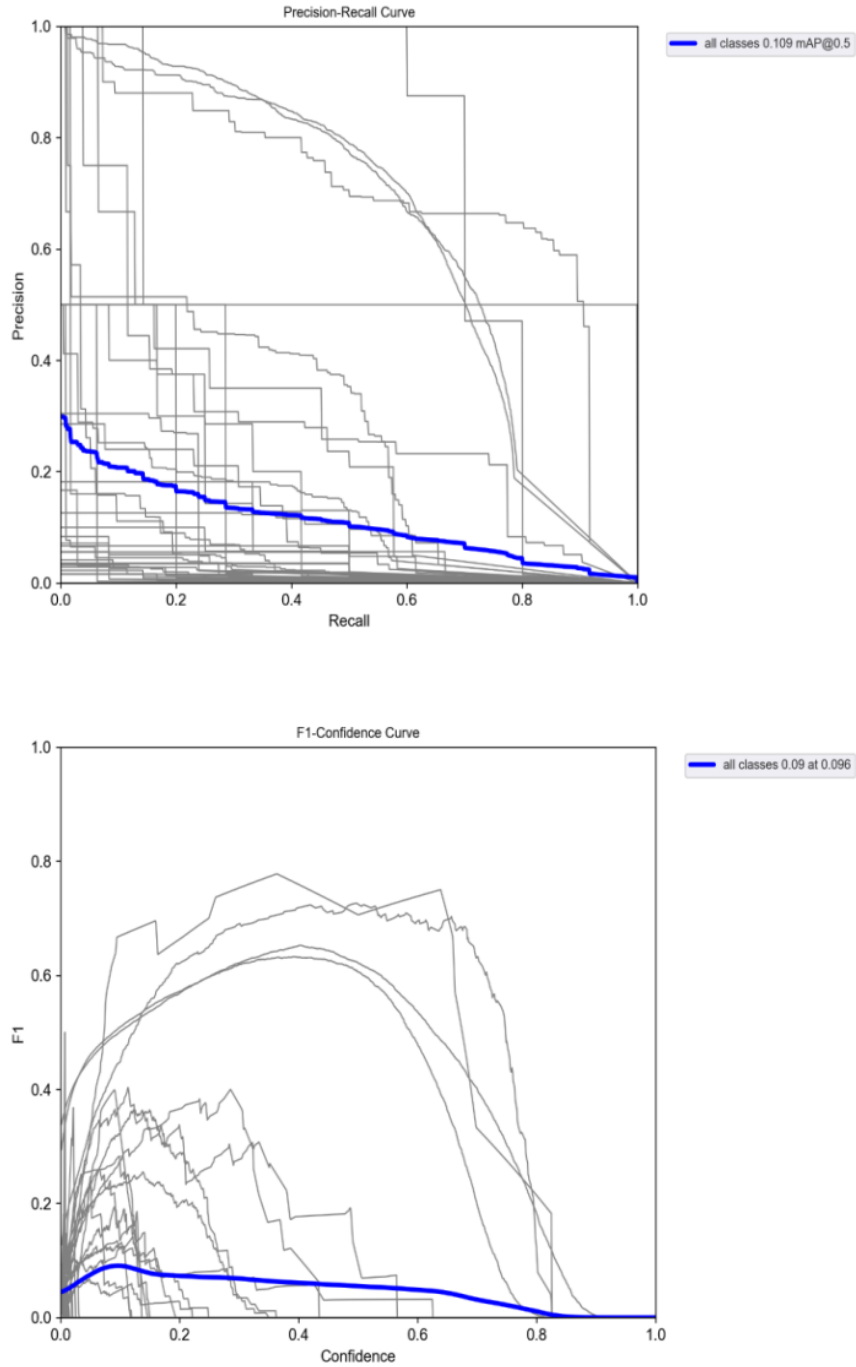


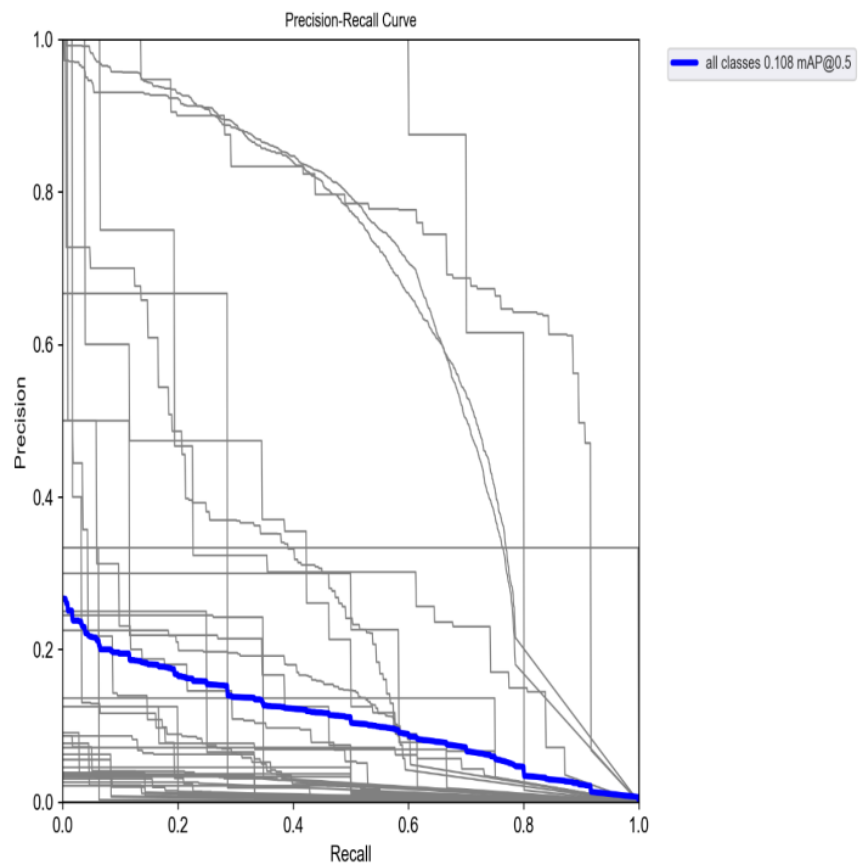
Fig 8: F1-Confidence curve of reduced warmup Fig 9: Precision- Recall curve of reduced warmup

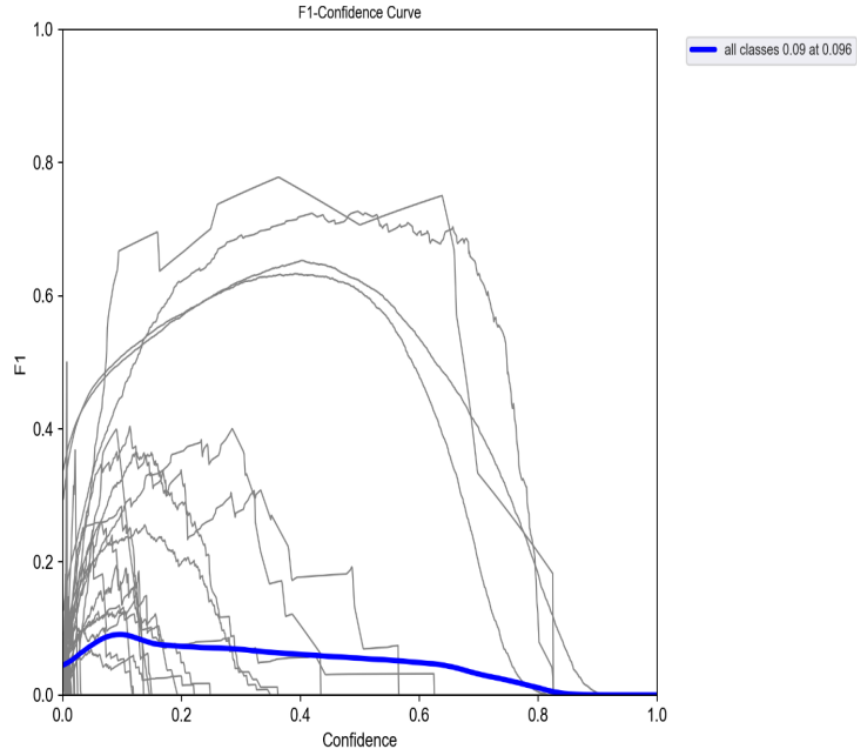
5.5 Increase the warmup momentum to 0.801

Case 5. Changing the value of warm-up momentum to 0.801

1. $lr0 \rightarrow 0.1$
2. $momentum \rightarrow 0.92$

3. $lrf \rightarrow 0.2$
4. $weight_decay: 0.0005$
5. $warmup_epochs \rightarrow 2.5$
6. $warmup_momentum \rightarrow 0.801$
7. $optimizer : SGD$





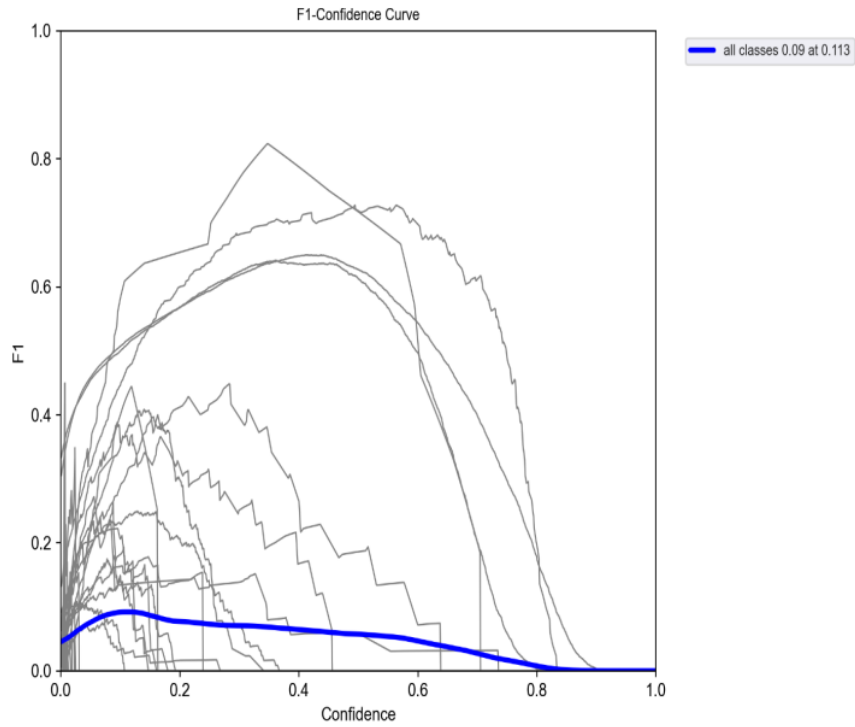
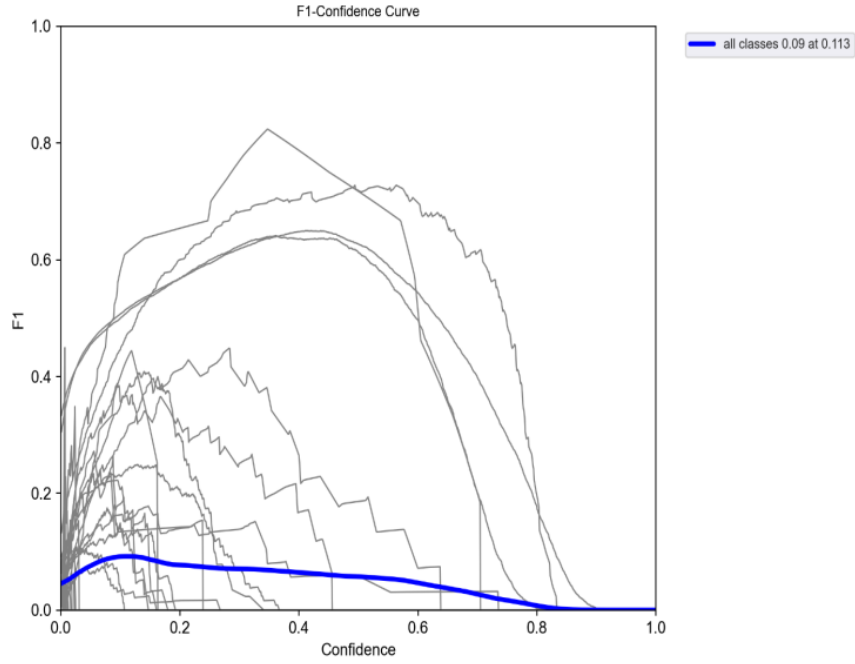
Reverted back to the best warmup epochs value that was found and increased the warmup momentum to 0.801 to see if performance can be improved. The result achieved was PR AUC 0.108 at mAP@0.5 | F1 max 0.09 at 0.096 confidences and was not able to improve upon the performance. Figure 10 shows the F1-Confidence curve which depicts the score of F1 max 0.09 at 0.096 confidence rate which is very less as compared to the result achieved using SGD optimizer. Figure 11 shows the Precision- Recall curve which depicts the score of PR AUC 0.108 at mAP@0.5 which is very less as compared to the result achieved using SGD optimizer.

Fig 10. F1-Confidence Curve for momentum 0.08 Fig 11. Precision- Recall curve momentum 0.08

5.6 Decreasing the weight decay to 0.000499

Case 6: decreasing the weight decay parameter

1. *lr0* -> 0.1
2. *momentum* -> 0.92
3. *lrf* -> 0.2
4. *weight_decay*: 0.000499
5. *warmup_epochs* -> 2.5
6. *warmup_momentum* -> 0.801
7. *optimizer* : SGD



In this experiment, we decrease the weight decay of our model to 0.000499. The result obtained was AUC 0.111 at mAP@0.5 | F1 max 0.09 at 0.113 confidence conducted with 30 epochs on the sub-sampled tiles of xView Dataset. The experiment was successfully able to improve upon the performance. Figure 12 and

Figure 13 shows the F1-Confidence and Precision- Recall curve respectively which depicts the score of AUC 0.111 at mAP@0.5 which is comparatively better result as compared to the results achieved. With the best weight decay of 0.000499 and decrease the warmup bias learning rate to 0.099 in order to verify if decreasing the warmup bias learning rate helps in getting better results. The result obtained was PR AUC 0.109 at mAP@0.5 | F1 max 0.08 at 0.099 confidence. The experiment was not able to improve upon the performance.

Fig 12. F1-Confidence curve for weight decay Fig 13. Precision – Recall curve for weight decay

5.8 Increase the warm up bias to 0.101

Case 7. Increase the warmup bias to 0.101

1. *lr0* -> 0.1
2. *momentum* -> 0.92
3. *lrf* -> 0.2
4. *weight_decay*: 0.000499
5. *warmup_epochs* -> 2.5
6. *warmup -momentum* -> 0.801
7. *warmup-bias* -> 0.101
8. *optimizer* : SGD

In this experiment, we revert back to our best weight decay and increase the warmup bias learning rate to 0.101. The result obtained was PR AUC 0.128 at mAP@0.5 | F1 max 0.09 at 0.116 confidence which successfully was an improvement to the model. Figure 15 shows the F1-Confidence curve which depicts the score of F1 max 0.09 at 0.116 confidence rate which is better as compared to the result achieved. Figure 16 shows the Precision- Recall curve which depicts the score of PR AUC 0.128 at mAP@0.5 which is better as compared to the result achieved. The result obtained was PR AUC 0.128 at mAP@0.5 | F1 max 0.09 at 0.116 confidence which successfully was an improvement to the model.

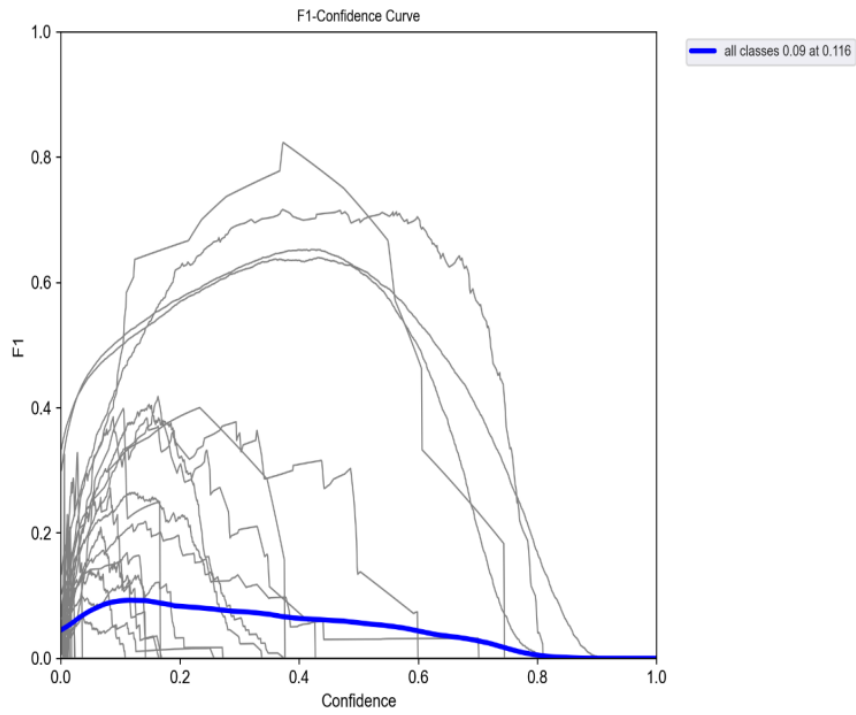
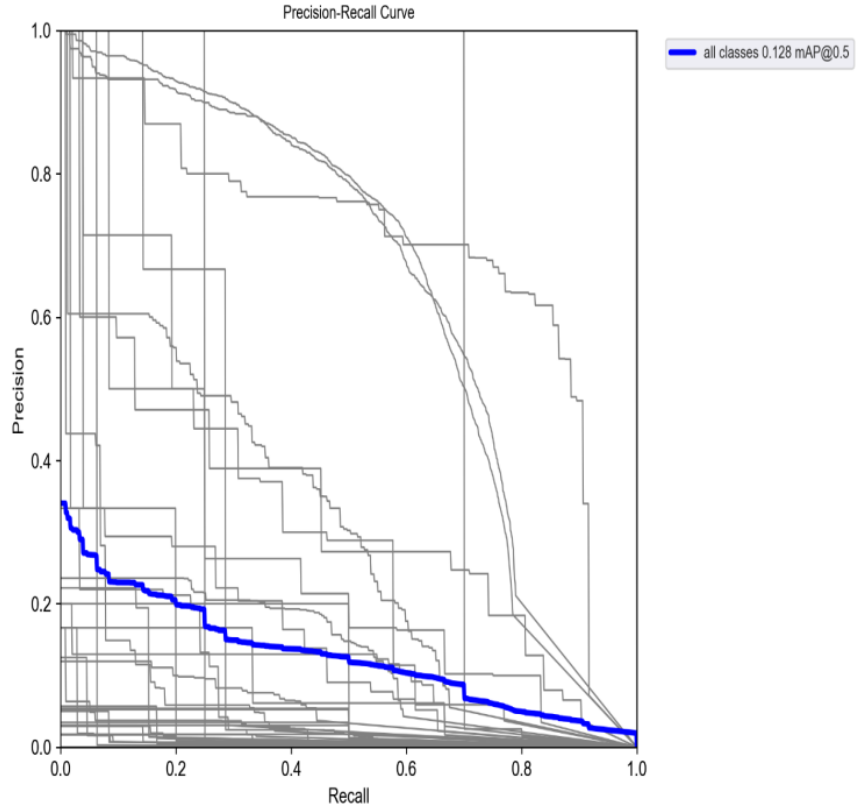


Fig 15. F1-Confidence curve for increased bias Fig16. Precision- Recall curve for increased bias

6. CONCLUSION & FUTURE WORK

Object detection includes basic tasks including object categorization, location, and segmentation. Object identification and related activities are divided into two groups: single stage and two stage. In this paper, we explored the single stage detection using YOLO V5 for object detection using xView Dataset. The paper examined single stage object detectors, particularly YOLO v 5, their architectural developments, underlying pre-trained CNN architectures. It also includes the several elements, optimizations, and tweaking of YOLO v5 hyper parameters, as well as all underlying combinations, in order to get the optimal model for improved identification of multi class objects.

Table 1 represents the summary of the experiments conducted with various combinations of the hyper-parameters tuned to evaluate all the different application scenarios. The best value for the parameters is mentioned in the table for the model. These experiments resulted in deciding the best combination of the hyper parameters and finalising the model for the best detection using the xView dataset. Similar experiments can be conducted with other versions of YOLO and tested on variety of data sets. By tuning the hyper parameters the model is fully exercised to give better results and suitably the best model with correct combination of hyper parameters and optimisers is achieved.

YOLOs are being used extensively in many real-time object tracking applications. Convolutional neural network advancements should be extensively tested in order to enhance single stage object detectors. Depending on the type of applications and underlying datasets, various algorithms may be utilized to further optimise the process.

Serial No.	Exp No.	Parameters Used	PR AUC at mAP@0.5	Max F1 Achieved @IOU
1	1	Baseline SGD w/ LR 0.01	0.105	0.09 @0.114
2	2	Baseline Adam w/ LR 0.001	0.043	0.03 @0.071
3	3	SGD Momentum @0.9	0.089	0.07 @0.133
4	4	SGD Momentum @0.905	0.088	0.07 @0.153
5	5	SGD Momentum @0.91	0.094	0.07 @0.148
6	6	SGD Momentum @0.92	0.104	0.08 @0.106
7	7	SGD Warmup Epochs @2.5	0.109	0.09 @0.095
8	8	SGD Warmup Epochs @2.4	0.105	0.08 @0.125
9	9	SGD Warmup Momentum @0.801	0.108	0.09 @0.096
10	10	SGD Warmup Momentum @0.799	0.107	0.09 @0.1
11	11	SGD Weight Decay @0.000499	0.111	0.09 @0.113
12	12	SGD Weight Decay @0.000498	0.101	0.08 @0.09
13	13	SGD Warmup Bias LR @0.099	0.109	0.08 @0.099
14	14	SGD Warmup Bias LR @0.101	0.128	0.09 @0.116
15	15	SGD Warmup Bias LR @0.102	0.107	0.08 @0.094



Figure 17. Predicted output of the objects

7 References

1. Laban, N. et al, 2019, December. Convolutional Neural Network with Dilated Anchors for Object Detection in Very High Resolution Satellite Images. In 2019 14th International Conference on Computer Engineering and Systems (ICCES). IEEE.
2. Z. -Q. Zhao, P. Zheng, S. -T. Xu and X. Wu, "Object Detection With Deep Learning: A Review," in *IEEE Transactions on Neural Networks and Learning Systems* , vol. 30, no. 11, pp. 3212-3232, Nov. 2019, doi: 10.1109/TNNLS.2018.2876865.
3. M. M. Rahman, S. Chakma, D. M. Raza, S. Akter and A. Sattar, "Real-Time Object Detection using Machine Learning," *2021 12th International Conference on Computing Communication and Networking Technologies (ICCCNT)* , 2021, pp. 1-5, doi: 10.1109/ICCCNT51525.2021.9580170.
4. Pedro F. Felzenszwalb, Ross B. Girshick, David McAllester and Deva Ramanan, "Object Detection with Discriminatively Trained Part-Based Models", *IEEE transactions on pattern analysis and machine intelligence* , vol. 32, no. 9, pp. 1627-1645, 2010
5. T. Ye, Z. Zhang, X. Zhang and F. Zhou, "Autonomous Railway Traffic Object Detection Using Feature-Enhanced Single-Shot Detector, ", *IEEE Access* , 2020
6. Y. Xu, H. Chen, C. Du and J. Li, "MSACon: Mining Spatial Attention-Based Contextual Information for Road Extraction", *IEEE Transactions on Geoscience and Remote Sensing* .
7. Shaoqing Ren, Kaiming He, Ross Girshick and Jian Sun, "Faster R-CNN: Towards Real-Time Ob-

- ject Detection with Region Proposal Networks”, *IEEE transactions on pattern analysis and machine intelligence*, vol. 39, no. 6, pp. 1137-1149, 2017.
8. T. -H. Wu, T. -W. Wang and Y. -Q. Liu, ”Real-Time Vehicle and Distance Detection Based on Improved Yolo v5 Network,” *2021 3rd World Symposium on Artificial Intelligence (WSAI)*, 2021, pp. 24-28, doi: 10.1109/WSAI51899.2021.9486316
 9. L. Aziz, M. S. B. Haji Salam, U. U. Sheikh and S. Ayub, ”Exploring Deep Learning-Based Architecture Strategies Applications and Current Trends in Generic Object Detection: A Comprehensive Review”, *IEEE Access*, vol. 8, pp. 170461-170495.
 10. J. Ge, B. Zhang, C. Wang, C. Xu, Z. Tian and L. Xu, ”Azimuth-Sensitive Object Detection in Sar Images Using Improved Yolo V5 Model,” *IGARSS 2022 - 2022 IEEE International Geoscience and Remote Sensing Symposium*, 2022, pp. 2171-2174, doi: 10.1109/IGARSS46834.2022.9883072
 11. B. Cui, Y. Zhang, J. Li and Z. Liu, ”Unmanned Aerial Vehicle (UAV) Object Detection in High-Resolution Image Based on Improved YOLO v5,” *CIBDA 2022; 3rd International Conference on Computer Information and Big Data Applications*, 2022, pp. 1-4.
 12. Wu, H et al., 2015, October. Typical target detection in satellite images based on convolutional neural networks. In 2015 IEEE International Conference on Systems, Man, and Cybernetics (pp. 2956-2961). IEEE. M.
 13. Song, Z., et al, 2014, May. Automatic ship detection for optical satellite images based on visual attention model and LBP. In 2014 IEEE Workshop on Electronics, Computer and Applications (pp. 722-725). IEEE.
 14. Zhang, Z. Shi, and J. Wu, ”A hierarchical oil tank detector with deep surrounding features for high-resolution optical satellite imagery,” *IEEE Journal of Selected Topics in Applied Earth Observations and Remote Sensing*, vol. 8, no. 10, pp. 4895–4909, 2015.
 15. Q. Luo and Z. Shi, ”Airplane detection in remote sensing images based on object proposal,” in 2016 IEEE International Geoscience and Remote Sensing Symposium (IGARSS). IEEE, 2016, pp. 1388–1391
 16. J. Lee, J. Wang, D. Crandall, S. Sabanovic, and G. Fox, ”Real-time object detection for unmanned aerial vehicles based on cloud-based convolutional neural networks,” in Proc. IEEE International Conference on Robotic Computing (IRC). Taichung, Taiwan. doi, vol. 10, 2017.
 17. Chi, H., et al, 2019, July. Multi-target Detection for Aerial Images Based on Fully Convolutional Networks. In 2019 Chinese Control Conference (CCC) (pp. 8801-8806). IEEE.
 18. R. A. Marcum, C. H. Davis, G. J. Scott, and T. W. Nivin, ”Rapid broad area search and detection of chinese surface-to-air missile sites using deep convolutional neural networks,” *Journal of Applied Remote Sensing*, vol. 11, no. 4, p. 042614, 2017.
 19. Polat et al., 2019, April. Aircraft Detection from Satellite Images Using ATA-Plane Data Set. In 2019 27th Signal Processing and Communications Applications Conference (SIU) (pp. 1-4). IEEE.
 20. Yao, Q et al., 2020. Multiscale Convolutional Neural Networks for Geospatial Object Detection in VHR Satellite Images. *IEEE Geoscience and Remote Sensing Letters*, 18(1), pp.23-27.